

# Copper plating on titanium alloy 6-2-4-2 using an in situ high voltage pulse followed by plate-up

R. J. von Gutfeld · Alan C. West

Received: 2 July 2007 / Revised: 29 October 2007 / Accepted: 1 December 2007 / Published online: 14 December 2007  
© Springer Science+Business Media B.V. 2007

**Abstract** We have used an in situ technique that removes the oxide from the surface of the alloy titanium 6-2-4-2, followed by copper electroplating of the surface. The oxide removal is accomplished by means of a short voltage pulse from a discharging capacitor between the cathode (titanium) and anode while submerged in the plating solution. Within seconds thereafter, the electrodes are switched to a separate power supply for electroplating copper onto the titanium. From the experimental data, we believe that the oxide is removed by means of dielectric breakdown mechanisms giving rise to a statistical probability that all of the surface oxide is removed. When this occurs, we obtain adherent depositions based on standard tape testing of the deposit. We determine a set of voltage and energy density conditions which are most likely to result in good adhesion. Scanning electron micrographs of adherent copper deposits are presented.

**Keywords** Titanium · Electroplating · In situ · Oxides · Breakdown · Copper

## 1 Introduction

Recently, we reported a novel method of electroplating copper on thin coupons of stainless steel 316 using a voltage pulse applied between anode and cathode (substrate) to remove the inhibiting oxide layer while the electrodes are submerged in the copper electrolyte [1]. This in situ method avoids the use of harsh chemicals often

required to eliminate inherent metal oxides prior to electroplating. At the same time, the new process eliminates some of the time consuming steps generally required to remove the oxide as well as to activate the metal surface. We purposely avoided chemical cleaning in the present experiments in order to investigate the feasibility of the very simple in situ oxide removal technique as it applies to a material having well known industrial applications. Aside from avoiding harsh chemicals for localized oxide removal, the present in situ method is also the least time consuming, requiring only on the order of 100 ms for the removal process. The present work reports results on the in situ plating of titanium 6-2-4-2 alloy using the voltage technique described in [1]. The alloy composition includes nominally 6% Al, 2% Sn, 4% Zr and 2% Mo by weight. Ti 6-2-4-2 has important applications for gas turbine compressor components, such as blades, discs and impellers in addition to engine afterburner structures. It is therefore of particular importance in the aerospace industry for its favorable physical and mechanical properties. However, nickel and/or nickel boron plating is often required to prevent spalling and erosion of the titanium surface in many of these applications. In order to achieve effective plating, the natural oxide of Ti 6-2-4-2 must first be removed, a procedure which has proved difficult to achieve in an environmentally friendly manner. In particular, it is desirable to avoid the use of hydrofluoric acid (HF) for both safety and environmentally safe disposal methods. While nickel and nickel boron are commonly plated onto the titanium alloy, the present work concentrates on in situ plating of copper on the Ti alloy in order to allow for a comparison of these results with those previously reported for similar work on stainless steel 316 [1]. The reason for studying copper on the titanium alloy is solely for the purpose of testing the generality of our in situ process on a

R. J. von Gutfeld (✉) · A. C. West  
Department of Chemical Engineering, Columbia University,  
500W. 120th St., New York, NY 10027, USA  
e-mail: rjv2104@columbia.edu

metal other than stainless steel 316. It is not intended that the copper on titanium be used for a nickel overlay. We recognize that titanium is directly plated with nickel for aerospace applications. Work to deposit the Ti alloy with nickel, using our in situ method, is in progress.

## 2 Experimental details

The experimental arrangement comprises a container containing an acid copper electrolyte with partially submerged electrodes consisting of a copper anode and the Ti 6-2-4-2 sample, the cathode (Fig. 1). Electrode spacing varied between 0.5 and 1 cm. The electrodes were connected by way of several switches to capacitors ranging in value from 300 to 5,000  $\mu\text{F}$ . A variable DC high voltage source with a maximum output of 300 V was used to charge one or more capacitors connected in parallel. During the capacitor charging cycle, the anode and cathode were disconnected from the rest of the circuit via open switches 2 and 3. Subsequently, the capacitor was discharged through the electrolyte between anode and cathode with switch 1 in the open position while closing switch 2. The temporal voltage pulse between anode and cathode was monitored and recorded by the storage oscilloscope (Agilent DSO 6012A). Subsequently switch 3 was closed to provide plate-up of the sample (cathode) with switches 1 and 2 in the open position. A second input to the oscilloscope was connected across a 1- $\Omega$  'dropping resistor' in series with the capacitor, anode–cathode circuit in order to obtain the circuit current. The voltage drop across the 1- $\Omega$

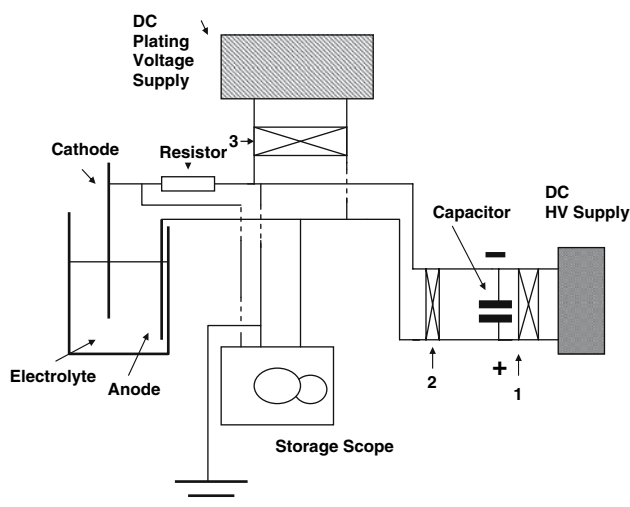


**Fig. 1** Experimental setup showing the cathode (Ti sample) partially immersed in the copper sulfate solution. Shown also are the high voltage charging supply to charge the capacitors, the storage oscilloscope, a switch for discharging the capacitors, a DC supply for plate-up following the capacitive discharge and a dropping resistor to measure the current during discharge

resistor is numerically equal to the current during capacitive discharge by Ohm's Law. That voltage is subtracted from the total voltage to ascertain the net anode–cathode voltage. However, with some exceptions (namely at the lowest capacitor voltages, e.g., Fig. 2) the current drops rapidly from its initial peak so the resistor voltage drop is generally negligible (e.g., Fig. 3) compared to the voltage drop between anode–cathode and therefore can be neglected in calculating the energy dissipation between anode and cathode.

After oxide removal, the samples were plated in the identical bath in which oxide removal occurred, typically for 4–10 min, using an Agilent E3632A DC power supply operated in the constant current mode. In this process step, switch 1 and 2 were in the open position with switch 3 in the closed position. The plating currents varied from  $\sim 10$  to 20  $\text{mA cm}^{-2}$  from sample to sample.

The Ti alloy was provided by Tyco Electronics Division in the form of 20-mil thick sheets from which we cut small coupons of the order of  $2 \times 0.5$  cm. Cleaning consisted in boiling the samples in water with a small amount of Alconox<sup>TM</sup> detergent for  $\sim 10$  min. This was followed by a water rinse, sonification in acetone followed by a second water rinse, sonification in ethanol followed by a final water rinse. Sample surface roughness was measured with a profilometer and found to be  $\pm 1.5$   $\mu\text{m}$  in height, with a lateral repetition of the order of  $\sim 20$   $\mu\text{m}$ . The acid copper electrolyte had the following composition: 240 mM copper sulfate, 1.8 M sulfuric acid, 50 ppm HCl. The anode was 100- $\mu\text{m}$  thick copper foil, typically between 0.5 and 1.0 cm in width.

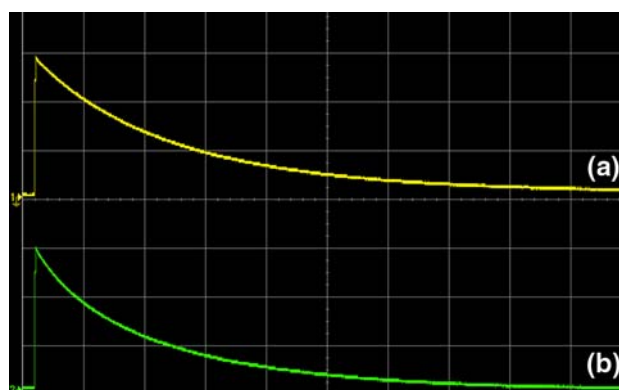


**Fig. 2** In situ voltage and current traces as a function of time for a pulse voltage applied across anode and cathode of a Ti 6-2-4-2 alloy sample prior to electroplating. The effective peak voltage (a) of the capacitor is  $\sim 60$  V, 20 V/major division, the peak voltage across the 1- $\Omega$  resistor, (b) is  $\sim 30$  V, equivalent to 30 A, 10 V/major division, the time scale, 5 ms/major division. The voltage (a) and current (b) both decay approximately exponentially. Copper electroplating after the voltage pulse resulted in an adherent deposition

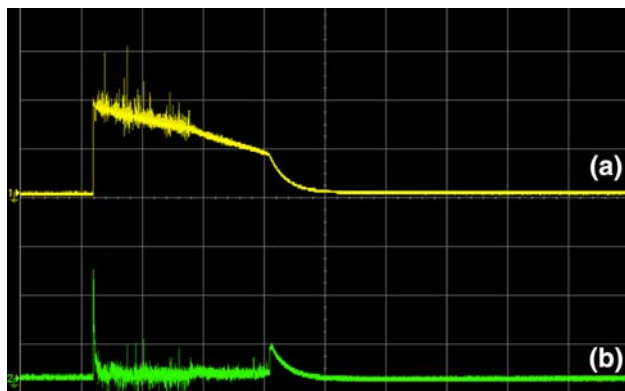


**Fig. 3** Voltage and current traces similar to those obtained in Fig. 2 except here using a capacitor voltage of 100 V. This higher voltage, trace (a) compared to that of Fig. 2, causes ionization and boiling of the electrolyte resulting in non-exponential decay with considerable noise. The corresponding current, indicated in terms of the voltage trace measured across the 1- $\Omega$  resistor, (b), has a sharp initial peak followed by almost no current flow due to the high resistance resulting in part from local boiling of the electrolyte. A return to quiescence of the electrolyte gives rise to a near exponential decay in both traces. The time scale is 50 ms/major division, vertical, (a) 50 V/major division, (b) 20 V/major division. Copper electroplating after the voltage pulse resulted in an adherent deposition

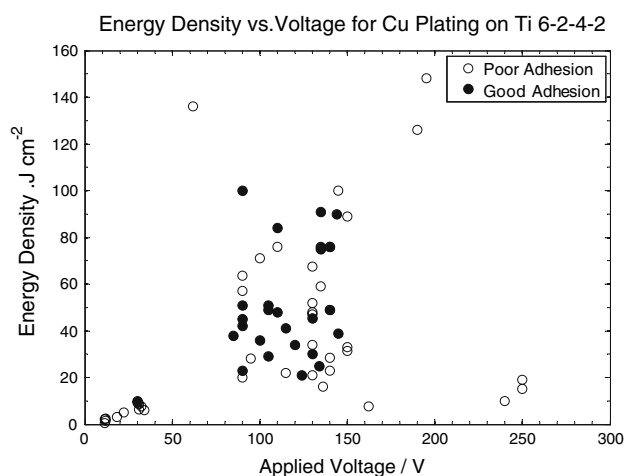
### 3 Experimental results

Figure 2 exhibits traces from an in situ voltage pulse, (a) of 60 V applied between anode and the combination of the dropping resistor and the submerged Ti 6-2-4-2 sample (cathode) in the copper sulfate solution. Simultaneously, the voltage (current) pulse (b) was monitored across the 1- $\Omega$  dropping resistor, as shown schematically in Fig. 1 by way of a second input to the digital storage scope. Both the voltage decay (a) and current decay (b) are well behaved and resemble an exponential though there is some deviation from a true RC exponential decay. This deviation is likely due in part to the parallel resistance and capacitance of the double layer as well as a time dependent electrolyte resistivity due to heating from the initial high current pulse. In Fig. 2, assuming an approximately exponential decay, we find the RC time constant to be  $\sim 10$  ms. Therefore, with the 5,000  $\mu\text{f}$  capacitor used to supply the discharge voltage, the nominal total circuit resistance,  $R$ , is then calculated to be  $\sim 2 \Omega$ , consistent with that determined from Ohms law, i.e., 60 V/30 A. Similar well behaved decay curves were previously observed for voltages of this magnitude applied to stainless steel 316 (used as the cathode) described in 1. At capacitor voltages of 60 V and below, the copper electrolyte remains quiescent for the immersed cathode areas used both here and in [1]. In the present experiments these surface areas are of the order of 0.5  $\text{cm}^2$  while for the earlier experiments on stainless steel they are of the order of 1  $\text{cm}^2$ . The sample of Fig. 2 was

found to have good copper adhesion after plate-up based on tape testing.

In Fig. 3 the total circuit voltage (a) and voltage (current) (b) decay pulses are again recorded simultaneously, using dual oscilloscope inputs for the pulse applied from the 5,000  $\mu\text{f}$  capacitor, here initially charged to  $\sim 100$  V. Traces a, b in Fig. 3 differ substantially from traces a, b, of Fig. 2 and typical for most sample data recorded in Fig. 4. At the higher voltages, the traces are noisy and follow a complicated decay, in contrast to those observed in Fig. 2. The differences are interpreted in terms of several non-equilibrium effects occurring in the electrolyte due to the higher voltage discharge consisting of (1) ionization of the electrolyte, observable as a blue spark between the two electrodes, (2) an audible shock wave accompanying the discharge and (3) local turbulence due to boiling of the electrolyte. During the interval in which local boiling occurs, the voltage discharge, trace (a) in Fig. 3 is relatively slow and very little (though non-zero) current, trace (b), flows, except for an initial spike, as the effective circuit impedance is high, in part due to bubble formation. After  $\sim 150$  ms, the electrolyte cools by means of thermal diffusion and fluid stirring to become quiescent. The effective circuit impedance is then once more relatively low ( $\sim 2 \Omega$ ) and both voltage and current decays resume with small, near exponential, relatively noise-free components.

A summary of data representing samples with ‘good’ and ‘poor’ (failed) adhesion is shown in Fig. 4. The data are displayed in terms of the energy density, ( $\frac{1}{2}CV^2$ ) incident on the immersed sample surfaces, versus the initial



**Fig. 4** A compilation of samples made under varying pulse voltages and energy density conditions. Adhesion was not obtainable at either the lowest or highest discharge voltages. Details are found in the discussion section. The voltage is the capacitor discharge voltage, corrected for the dropping resistor where necessary, the energy per unit area is based on the effective discharge voltage existing between anode and cathode

voltage,  $V$ . Here  $V$  is defined as the peak value of the storage scope voltage (ignoring the dropping resistor voltage as previously described except for low voltages where  $V$  has been adjusted to account for the series dropping resistor voltage which must be subtracted from the storage scope voltage) at the start of the discharge of capacitor,  $C$ . The energy density is divided by the immersed front and back sample areas. The rationale for dividing the energy equally between both front and back sample surfaces arises from the fact that copper deposition is generally found on both faces adherent or not adherent. That both surfaces are plated is consistent with our voltage mapping of the electrolyte as a function of position (with electrodes in place) yielding a nearly uniform voltage (electric field) distribution throughout the electrolyte. At capacitor voltages greater than  $\sim 150$  V, copper depositions were never found to be adherent, partly due to the large fraction of the capacitor energy dissipated in the electrolyte. At the same time, there is intense boiling of the solution which results in extremely poor electrical contact between anode and cathode. This likely prevents removal of the oxide due both to the lack of a high electric field across the oxide and very little current flow due to the high impedance of the circuit. With these assumptions, in conjunction with the previous discussion of the voltage–current traces of Figs. 2 and 3, the minimum initial current that gives rise to successful plating for surface areas of  $\sim 0.5$  cm<sup>2</sup> is  $\sim 30$  A with a maximum  $\sim 75$  A.

Each of the samples in Fig. 4 was subjected to the standard Scotch™ tape test, both in the pull (upward) and shear (tangential) directions. The criterion for ‘good’ adhesion requires that no copper be removed by both pull and shear test. Some samples were subjected to both tests up to seven times without copper removal though for most samples this test was undertaken only one to two times to ascertain good adhesion. The distribution of samples with good and poor adhesion under similar conditions is described in terms of an approximate model in the last section. Generally, we believe good adhesion occurs when substantial sample oxide is removed by way of the in situ discharge pulse to cause dielectric breakdown. The breakdown is initiated by way of the high electric field across the oxide caused by the electrical discharge followed by a short period of intense oxide heating by way of a pulsed high current, also known as a thermal runaway process [2–9]. Figure 4 indicates a voltage lower limit of  $\sim 25$ – $30$  V (between anode and cathode) below which no samples are found to have an adherent or uniform copper deposit after plate-up. On the other hand, all samples subjected to a discharge voltage pulse of at least  $\sim 50$  V were found to result in a uniform copper deposition of substantial thickness after plate-up, but with only some of these deposits resulting in good adhesion. Control samples,

not subjected to any discharge voltage, result in only a very thin, and irregular copper deposit upon plate-up, sufficiently thin such that the substrate surface is visible through the deposition. It is therefore, evident that the in situ discharge plays a significant role in overcoming the tenacious oxide on the titanium alloy surface. Typically, samples with small areas, on the order of  $0.2$ – $0.8$  cm<sup>2</sup>, are found to have a greater probability of adherent copper for pulse voltages higher than  $\sim 60$  V. In general we have not been able to predict good adhesion based on the shape of the voltage and current decay curves. It should be noted that all the voltage discharges were cathodic, i.e., the sample was connected to the negative side of the capacitor in order to obtain copper deposition. Attempts to obtain plating using anodic pulses for stripping the oxide failed, possibly for several reasons; application of an anodic pulse drives oxygen to the Ti possibly causing additional titanium oxide to form. In addition, more time is required in re-arranging the leads for the cathodic plating after an anodic discharge, possibly leading to additional oxidation of the cathode surface during that interval. On the other hand, cathodic pulses (a) promote hydrogen evolution which may help in chemically reducing the Ti oxide, (b) promote Cu ions to migrate to the Ti cathode prior to plate-up, (c) help to prevent re-oxidation as there is a very small time interval between the capacitive discharge and the plate-up step.

Micrographs of an in situ copper plated Ti 6-2-4-2 sample are displayed at two magnifications in Fig. 5a, b. The copper deposit was obtained using an effective capacitive discharge of 90 V, while the combined front and back plated surface areas are  $0.45$  cm<sup>2</sup>. After the discharge, the plate-up of copper was undertaken for 7.5 min with a current density of  $22$  mA cm<sup>-2</sup>. With these plating parameters, the estimated thickness of the deposit is  $\sim 3.5$  μm. Tape pull and shear tests were applied twice on both front and back surfaces indicating ‘good’ adhesion. The film appears continuous in both micrographs taken at two magnifications. (Note, each minor tick mark on the micrograph is 1/10 that of the printed scale.) Figure 5a, taken at low magnification indicates that the in situ plating process can be used effectively to obtain relatively large areas without defects in the form of holes or bare (non-plated) regions. Figure 5b, taken at a higher magnification indicates some layering consisting of larger crystallites. This type of morphology is consistent with the overall sample surface roughness previously discussed.

#### 4 Discussion

The scatter observed in our adhesion data for Ti samples (Fig. 4) subjected to similar capacitive discharge

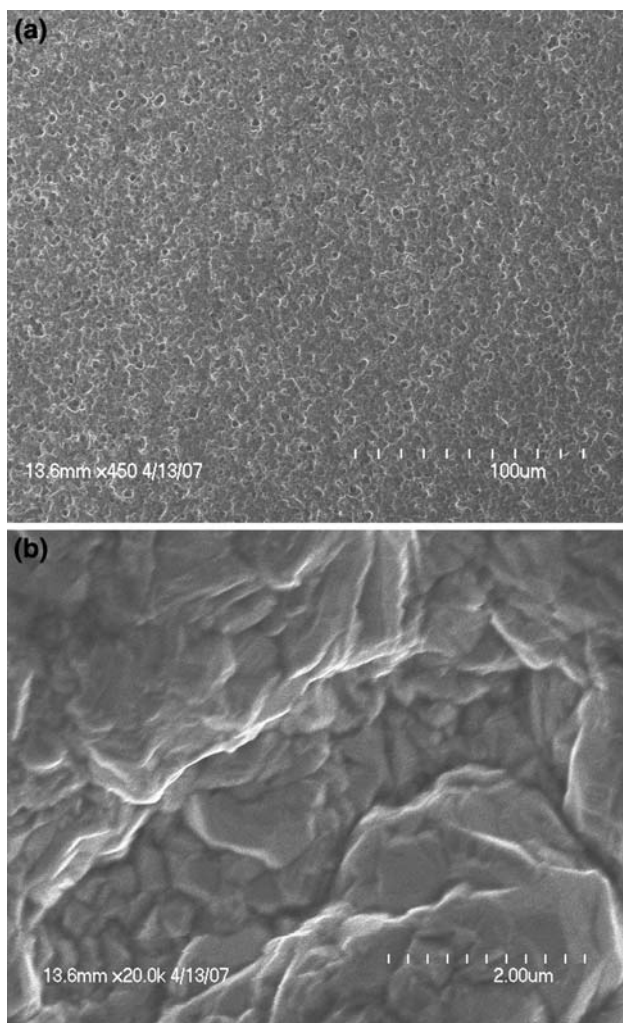


**Fig. 5** (a, b) Scanning micrographs of a copper film on Ti 6-2-4-2 taken at two magnifications. Note, the printed scale in microns equals the length of the 10 minor subdivisions

conditions prior to plate-up is probably related mainly to the mechanisms leading to dielectric breakdown. Without the breakdown of the inhibiting oxide layer, electroplating of copper is not possible. Partial oxide removal leads to poor adhesion of any electroplated deposition. For a 4-nm thick Ti oxide film, the average electric field for a 100 V discharge pulse is  $\sim 2.5 \times 10^8 \text{ V cm}^{-1}$ , neglecting losses in the electrolyte and the dropping resistor. This high electric field must certainly result in dielectric breakdown, but the breakdown may be very localized and therefore not result in complete oxide elimination across the entire surface of the substrate. The randomness of the breakdown is affected by naturally occurring random or statistical non-uniformities or flaws such as weak spots in the dielectric as well as variations in the substrate surface. The results for titanium differ substantially from those previously found for stainless steel 316. For a range of stainless steel material thicknesses (50–250  $\mu\text{m}$ ) and discharge voltages

between  $\sim 25$  and 200 V, adherent copper deposits resulted for almost all samples. This statistical contrast is consistent with the fact that titanium oxide is well-known to be an extremely robust, protective coating compared to iron oxide and chrome oxide expected to form on stainless steel 316. Therefore, Ti oxide can be expected to be more difficult to remove consistently and uniformly by our technique. Based on the present experiments, we find that no exchange plating occurs after application of the voltage pulse. Experiments to ascertain this were performed on both stainless steel 316 and Ti 6-2-4-2. Samples were examined immediately after breakdown (i.e., application of the voltage pulse). Another set of both stainless steel and titanium was examined after leaving the samples in the copper electrolyte for 60 s after application of the discharge pulse. In both cases, only a sludge was found on the samples which was readily wiped off with a Q-tip or paper towel.

Extensive studies on dielectric breakdown of oxides under varying conditions have been reported over the past several decades due to the importance of obtaining reliable thin oxide films used in high speed semiconductor devices. Such work has been stimulated by the need to obtain high dielectric films with low leakage currents for use in field effect transistors. This has led to numerous investigations of the dielectric breakdown of silicon and aluminum oxides using metal-oxide-semiconductor (MOS) structures of the kind used in field effect transistor gates [2–10]. MOS structures were used to investigate the electrical conduction and breakdown characteristics of aluminum oxide insulating thin films deposited on silicon by examining the current voltage behavior up to and including breakdown of the oxides [8]. From those measurements, it was possible to distinguish two distinct currents that can occur prior to dielectric breakdown, i.e., Fowler–Nordheim tunneling and Frenkel-Poole emission, the latter occurring just before breakdown. Ultra thin gate oxide breakdown has also been studied using metal oxide semiconductor structures (MOS) for oxides less than 4 nm where the permanent destruction of the oxide is determined from the resistor-like behavior of the current–voltage curves [9]. Based on the findings of various semiconductor breakdown studies, it has been proposed that high field voltage dielectric breakdown is a multi-step process consisting of (1) trap generation within the oxide, (2) local high currents through the oxide in addition to tunneling currents. For our system, we equate the electrolyte in contact with the oxide as one electrode of a capacitor. The oxide film is the capacitor dielectric in contact with the second electrode, the titanium substrate. The energy initially stored in the dielectric due to the application of the high electric field (initial portion of the high voltage pulse) causes the capacitor to break down in numerous closely separated locations. Finally, as the

capacitor continues to discharge, thermal runaway occurs which, in principle, destroys the remaining oxide together with the effect of electron injection into the oxide from the metal substrate. This final step leading to high current densities is also referred to in semiconductors as complete or hard breakdown [9, 10].

While thermal runaway is described as the final step in the destruction of any remaining dielectric, this process is not always sufficiently complete to provide an adequately uniform clean surface required for good adhesion for electro deposition. The runaway step results in an effectively complete short between metal and semiconductor in an MOS structure, but not necessarily the surface quality required for good electrodeposits. We believe this uneven surface quality (i.e., incomplete oxide removal) may explain the scatter found in Fig. 4 between ‘good’ and ‘poor’ adhesion on samples processed under similar conditions. In that regard, the theory of thin oxide statistics is helpful in understanding randomness of oxide breakdown that may occur, which in turn will lead to differences in the degree of oxide removal as a function of position on the sample surface. Various approaches have been applied to the theory of breakdown statistics in thin silicon oxide films using Monte Carlo simulations, percolation theory and a ‘cell’ model. In general, they describe a distribution of oxide failures or oxide breakdowns that occur under different conditions and varying oxide thicknesses. The results of such statistical models are referred to here only as feasible support for our statistical results without going into the details of the complex calculations found in the references [5, 10, 11].

## 5 Summary

It is possible to electroplate copper onto small coupons of titanium 6-2-4-2 using an in situ technique previously

described for stainless steel 316. The technique uses a short voltage pulse to remove the robust oxide while the titanium is immersed in the plating solution, making electroplating possible immediately thereafter. For some samples there appears to be incomplete oxide removal resulting in poor copper adhesion. We offer an explanation for the adhesion randomness from sample to sample in terms of incomplete dielectric breakdown of the oxide, based on a tunneling and thermal runaway model, well studied for oxides used in field effect transistors.

**Acknowledgments** We are pleased to acknowledge experimental help from Joseph Woo and are grateful for the titanium 6-2-4-2 samples provided us by Tyco Electronics Division, Harrisburg, PA.

## References

1. von Gutfeld RJ, West AC (2007) *J Vac Sci Technol A* 25(2):319; (see also von Gutfeld RJ, West AC in PCT patent application, WO 2006/086407, ‘In situ plating and etching of materials covered with a surface film’ August 17, 2006)
2. Klein N (1969) *J Electrochem Soc* 116:963
3. Lombardo S, Crupi F, La Magna A, Spinella C, Terrasi A, La Manita A, Neri B (1998) *J Appl Phys* 84:472
4. Klein N (1983) *Thin Solid Films* 100:335
5. Sune J (2001) *IEEE Electr Dev L* 22:296
6. Hickmott TW (2000) *J Appl Phys* 88:2805
7. Jackson JC, Robinson T, Oralkin O, Dumin DJ, Brown GA (1998) *J Electrochem Soc* 145:1033
8. Kolodzey J, Chowdhury EA, Adam TN, Qui G, Rau I, Olowolafe JO, Suehle JS, Chen Y (2000) *IEEE T Electron Dev* 47:121
9. Huang C-H, Hwu J-G (2001) *J Vac Sci Technol B* 19:1894
10. Sune J, Placencia I, Barnio N, Farres E, Marin Fr, Aymerich X (1990) *Thin Solid Films* 185:347
11. Sune J, Wu EY (2003) *IEEE Electr Device Lett* 24:272